

Cite this article as: Iablonskii P, Cebotari S, Tudorache I, Granados M, Morticelli L, Goecke T *et al.* Tissue-engineered mitral valve: morphology and biomechanics. *Interact CardioVasc Thorac Surg* 2015; doi:10.1093/icvts/ivv039.

## Tissue-engineered mitral valve: morphology and biomechanics<sup>†</sup>

Pavel Iablonskii\*, Serghei Cebotari, Igor Tudorache, Marisa Granados, Lucrezia Morticelli, Tobias Goecke, Norman Klein, Sotirios Korossis, Andres Hilfiker and Axel Haverich

Department of Cardiothoracic, Transplantation and Vascular Surgery (HTTG) Hannover Medical School, Hannover, Germany

\* Corresponding author. Medizinische Hochschule Hannover, Klinik für Herz-, Thorax-, Transplantations- und Gefäßchirurgie. OE 6210, Carl-Neuberg-Straße 1 30625 Hannover, Germany. Tel: +49-176-15326429; fax: +49-511-5325404; e-mail: yablonski.pavel@mh-hannover.de; pavel.yablonski@gmail.com (P. Iablonskii).

Received 16 September 2014; received in revised form 25 January 2015; accepted 4 February 2015

### Abstract

**OBJECTIVE:** The present study aimed at developing tissue-engineered mitral valves based on cell-free ovine mitral allografts.

**METHODS:** The ovine mitral valves (OMVs) ( $n = 46$ ) were harvested in the local slaughter house. They were decellularized using detergent solutions and DNase. The effectiveness of decellularization was assessed by histological (haematoxylin-eosin, Movat's pentachrome) and immunofluorescent staining (for DNA and  $\alpha$ -Gal), and DNA-quantification. To reveal the receptiveness of decellularized tissue to endothelial cells (ECs), the valve leaflets were reseeded with ovine ECs, derived from endothelial progenitor cells *in vitro*. For assessment of biomechanical properties, uniaxial tensile tests were carried out.

**RESULTS:** Histology and immunofluorescent staining revealed absence of cell nuclei in decellularized leaflets, chordae and papillary muscles. According to the software for immunofluorescence analysis, reduction in DNA and  $\alpha$ -Gal was 99.9 and 99.6%, respectively. DNA-quantification showed 71.2% reduction in DNA content without DNase and 96.4% reduction after DNase treatment. Decellularized leaflets were comparable with native in ultimate tensile strain (native,  $0.34 \pm 0.09$  mm/mm, vs decellularized,  $0.44 \pm 0.1$  mm/mm;  $P = 0.09$ ), and elastin modulus (native,  $0.39 \pm 0.27$ , vs decellularized,  $0.57 \pm 0.55$ ,  $P = 0.46$ ), had increased ultimate tensile stress (native,  $1.23 \pm 0.35$  MPa, vs decellularized  $2.12 \pm 0.43$  MPa;  $P = 0.001$ ) and collagen modulus (native,  $5.5 \pm 1.26$ , vs decellularized,  $8.29 \pm 2.9$ ;  $P = 0.04$ ). After EC seeding, immunofluorescent staining revealed a monolayer of CD31-, eNOS- and vWF-positive cells on the surface of the leaflet, as well as a typical cobble-stone morphology of those cells.

**CONCLUSIONS:** Decellularization of ovine mitral valve results in a mitral valves scaffold with mechanical properties comparable with native tissue, and a graft surface, which can be repopulated by endothelial cells.

**Keywords:** Tissue engineering • Mitral valve • Mitral homograft

### INTRODUCTION

Mitral valve replacement is a last therapeutic option for patients unsuitable to mitral valve repair. Currently available mitral valve prostheses have major limitations, including life-long anticoagulation therapy for mechanical prosthesis, limited durability for biological prosthesis and disability to grow for both [1]. On the other hand, human cryopreserved pulmonary valve allografts have demonstrated optimal haemodynamics and reduced reoperation rate [2, 3]. In spite of this fact, the use of mitral valve homografts for mitral valve replacement has been reported occasionally. In 1971, Graham *et al.* [4] published promising results of fresh mitral homograft implantation, but later the mid- and long-term results of both fresh and cryopreserved mitral valve homografts were found

unsatisfactory [5]. Limited durability of the mitral homografts influenced reoperation rate and the long-term survival of the patients [6].

The recent developments in biotechnology and tissue engineering have the potential to create the new generation heart valve substitutes with increased durability when compared with conventional homografts and xenografts [7, 8]. However, none of artificial structures were successfully used in *in vivo* tests. On the other hand, decellularization of the homografts has been shown to reduce the graft immunogenicity and reoperation rates when used in aortic or pulmonary valve replacement [2, 3, 9–11].

To the best knowledge of the authors, there are no data available regarding decellularization of the mitral valve graft. The aim of this study was to establish a protocol for decellularization of the whole ovine mitral valve (OMV) allograft with a view to developing OMV scaffolds for subsequent implantation in the orthotopic ovine animal model in future studies, simulating the clinical homogeneous model. Part of the work in the present study also focused on the assessment of the effects of the developed

<sup>†</sup>Presented at the 8th Annual Meeting of the European Association for Cardio-Thoracic Surgery, Milan, Italy, 11–15 October 2014.

decellularization method on the morphological and biomechanical characteristics of OMV scaffolds.

## MATERIALS AND METHODS

### Valves harvesting

Whole OMVs ( $n = 46$ ) were harvested at the local abattoir immediately after the animal was slaughtered. The valves were stored in phosphate buffered saline [phosphate buffered saline (PBS); Sigma-Aldrich, St Louis, MO, USA] at 4°C for 4–6 h until being decellularized. The whole valves were harvested with a small rim of the left atrium (3–4 mm wide), chordae tendineae and papillary muscles. The mitral valve comprises two leaflets: the anterior and posterior. According to common nomenclature, the mitral leaflets can be divided into three zones, named A1, A2 and A3 (anterior leaflet) and P1, P2 and P3 (posterior leaflet). A1 and P1 are the lateral zones, A2 and P2 the middle ones and A3 and P3 the medial ones [12]. During the study, the A2 zone of each valve was used for cytotoxicity test, except for DNA-quantification, for which the A1 and A3 zones were used.

### Decellularization

Prior to decellularization, the whole OMVs were disinfected by washing in povidone iodide (Braunol®; B. Braun, Melsungen, Germany) for 5 min, followed by 20 min washing in PBS. The whole valves were subsequently decellularized using sodium deoxycholate (SD; Sigma-Aldrich, St Louis, MO, USA), sodium dodecyl sulphate (SDS ultrapure; Carl Roth, Karlsruhe, Germany) and  $\beta$ -mercaptoethanol ( $\beta$ -ME; AppliChem, Darmstadt, Germany). The detergent treatment was performed under constant shaking at room temperature:

- (i) Step 1—distilled water, 6 h;
- (ii) Step 2—0.2% SDS, 0.2% SD, 25 mM  $\beta$ -ME, 12 h;
- (iii) Step 3—0.3% SDS, 0.3% SD, 25 mM  $\beta$ -ME, 12 h;
- (iv) Step 4—0.4% SDS, 0.4% SD, 25 mM  $\beta$ -ME, 12 h;
- (v) Step 5—0.5% SDS, 0.5% SD, 25 mM  $\beta$ -ME, 12 h.

Thereafter DNA was cleaved with DNase I (24 h at room temperature under continuous shaking, 30000 IU DNase I per valve, 150 IU/ml, Sigma-Aldrich) using the previously described protocol [13]. Washing was performed in ten 12-h steps, two with distilled water and eight with PBS. The overall length of the decellularization process was 198 h.

### Cell culture

Endothelial progenitor cells (EPCs) were isolated from peripheral blood of an adult sheep using the previously described protocol [14]. Following isolation, the cells were transfected with a red fluorescent protein (RFP) expressing lentivirus [14]. Cell cultivation was performed in EBM-2 medium (Lonza, Basel, Switzerland) at 39°C and 5% CO<sub>2</sub>. The medium was changed every second day.

### Histological staining

A half of an A2 zone of each decellularized sample ( $n = 14$ ) was embedded in paraffin, sliced into 8  $\mu$ m-thick sections and stained by haematoxylin-eosin (H&E), Movat's pentachrome and van

Gieson stains. Slides were analysed using a routine bright field microscopy (Olympus BX40, Olympus, Tokyo, Japan; with colour camera AxioCam MRc, Carl Zeiss, Jena, Germany). Sections of an untreated valve were also stained and served as a positive control.

### Immunofluorescent staining

The other half of the A2 zone of each decellularized sample was snap-frozen in liquid nitrogen, mounted in Tissue-Tek (Sakura Finetek Europe, AV Alphen an den Rijn, Netherlands) and cut into 6- $\mu$ m-thick sections. The effectiveness of decellularization was assessed by the 4,6-diamidino-2-phenylindole dihydrochloride (DAPI) stain (Invitrogen, Carlsbad, CA, USA) and staining against the  $\alpha$ -Gal epitope (DyLight 594 Bandeiraea Simplicifolia Lectin I Isolectin B4, Vector Laboratories, Burlingame, Great Britain) ( $n = 14$ ). In order to assess the integrity of the basal membrane, immune stain against collagen IV (clone C122, DAKO, Hamburg, Germany) was performed ( $n = 3$ ). The endothelial phenotype of cells used for contact cytotoxicity testing was confirmed by CD31 (monoclonal mouse IgG<sub>2a</sub>, Serotec, Raleigh, North Carolina, USA), von Willebrand factor (polyclonal rabbit IgG, DAKO) and eNOS (monoclonal mouse IgG<sub>1</sub>, eNOS/NOS Type III, BD Transduction Laboratories, San Jose, CA, USA) immune stains ( $n = 8$ ).

For quantitative analysis of images obtained with fluorescent microscopy (AxioObserver A1, Carl Zeiss Microimaging, with camera AxioCamMRm, Carl Zeiss), a software developed in our department was used. The software is based on detecting and counting pixels of specific colour and intensity ranges on JPEG-files derived from fluorescence microscopy images. Thus subsequent comparison of pixel counts derived from different comparable representative pictures via histogram analysis enables conclusions concerning particular colour and intensity differences, respectively, increases and decreases.

### Contact cytotoxicity

The potential residual toxicity of SDS, SD and  $\beta$ -ME, was assessed by seeding 1.5 cm<sup>2</sup> samples from the A2 and P2 leaflet zones of eight decellularized valves with ovine ECs. Each sample was placed in a well of a 12-well plate and fixed with metal rings. The samples were then seeded with RFP-positive ECs at P9, derived from ovine endothelial progenitor cells (EPCs). Specifically, 2 ml of  $5 \times 10^4$  cells/ml cell suspension (EBM-2 medium; Lonza) was added to each well, resulting to a seeding density of  $3.2 \times 10^4$  cells/cm<sup>2</sup>. The cultivation was performed until the full confluence was reached. Pictures were taken every day using intravital microscopy under sterile conditions.

### Uniaxial tensile test

Native ( $n = 7$ ) and decellularized ( $n = 7$ ) leaflet samples were subjected to uniaxial tensile loading to failure using a Zwick Roell Z 0.5 device, fitted with a 200 N load cell (Zwick Roell AG, Ulm, Germany). The samples were isolated from the A2 zone of the leaflets, along the radial direction, and maintained an aspect ratio of 2:1 (length:width). Prior to testing, the thickness of each sample was measured with a digital thickness gauge (Sylvac S246, Sylvac SA, Crissier, Switzerland). All samples were tested using a preloading force of 0.005 N and 10 preconditioning cycles (strain level of 16%), prior to loading to failure. The resulting stress-strain behaviour of

the tested samples was analysed in terms of six parameters, including the ultimate tensile strength, transition stress, failure and transition strain, elastin phase modulus and the collagen phase modulus.

## DNA quantification

In order to further assess the extent of decellularization of the treated valves, the DNA content of native ( $n = 3$ ) and decellularized ( $n = 7$ ) leaflets was quantified using the DNeasyBlood&Tissue Kit (QIAGEN N.V., Venlo, Netherlands). Three fragments, 25 mg each, were excised from the A1 and A3 leaflet zones of each valve. The DNA was isolated according to the manufacturer's instructions, and quantified in a NanoDrop 1000 spectrophotometer (Thermo Scientific, Waltham, MA, USA).

## Statistics

All reported data were expressed as mean  $\pm$  SD. The paired Student's *t*-test was used for determining statistical significance, which was defined at the 0.05 level. The analysis was conducted in the STATISTICA 10.0 software package.

## RESULTS

### Decellularization

The completeness of the decellularization was demonstrated by the absence of whole nuclei in all three types of histological staining (Figs 1–3). The histological results also revealed a preserved four-layered leaflet structure, comprising the atrialis, spongiosa, fibrosa and ventricularis. There was no significant difference in the appearance of the elastin and collagen fibres, and glycosaminoglycans, as evaluated by Movat's Pentachrome, between the native and decellularized groups. Under Van Gieson staining, collagen and elastin in decellularized valves appeared to be organized in a layered order without any signs of disruption, similar to the native tissue. Similarly, DAPI and DyLight fluorescent staining showed 99.9%  $\pm$  0.064 ( $P < 0.05$ ) reduction in DNA and 99.63%  $\pm$  0.12 ( $P < 0.05$ ) reduction in  $\alpha$ -Gal, respectively (Fig. 4). Moreover, the collagen I fibres in the decellularized leaflets were organized in the same manner as in the native ones (Fig. 5), whereas collagen IV staining showed a superficial fluorescent layer over the entire leaflet surface (Fig. 6). The reduction of fluorescence intensiveness by 60% was determined.

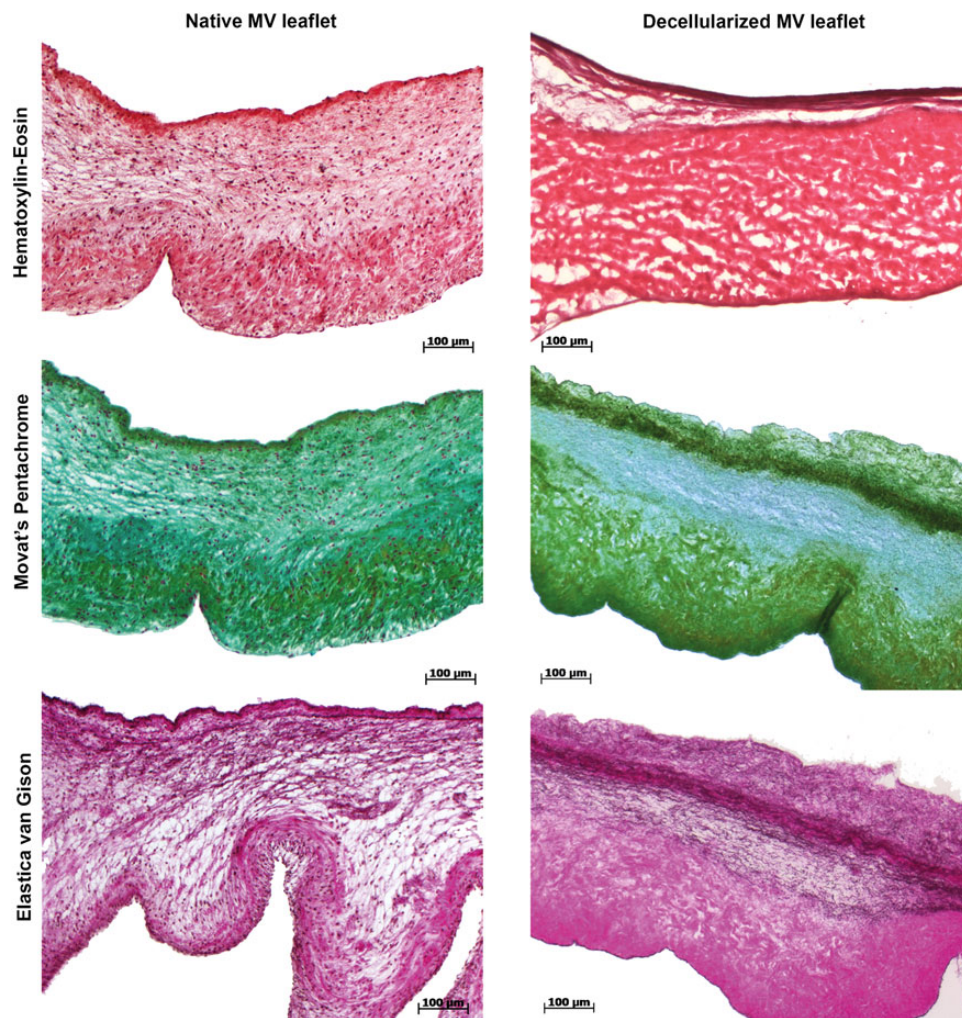


**Figure 1:** Bright-field microscopy of H&E, Movat's pentachrome and van Gieson staining of native (left) and decellularized (right) ovine MV leaflet. Decellularized leaflet lacks cell nuclei, but the structure of the extracellular matrix is unchanged.

## Contact cytotoxicity test

Cell growth was similar in all the decellularized leaflet samples tested, whereas full coverage of the leaflet surface was achieved after 5 days. Under intravital immunofluorescent microscopy, the RFP-positive cells demonstrated typical cobble-stone morphology. Moreover, immunofluorescence labelling revealed CD31-, eNOS- and vWF-positive cells, whereas H&E and Movat's Pentachrome stains demonstrated the presence of a continuous cell monolayer on the surface of the decellularized leaflets (Fig. 7).

## Uniaxial tensile testing

Although the decellularized leaflets tended to be thinner than the native ones ( $0.24 \pm 0.11$  mm and  $0.35 \pm 0.06$  mm, respectively),

the difference was statistically significant ( $P = 0.03$ ). With regard to the biomechanical parameters studied (Fig. 8), the differences in the transition stress, failure and transition strain and elastin phase modulus between the native and decellularized were not statistically significant ( $0.12 \pm 0.05$  MPa vs  $0.24 \pm 0.08$  MPa,  $P = 0.1$ ;  $0.34 \pm 0.09$  mm/mm vs  $0.44 \pm 0.1$  mm/mm,  $P = 0.08$ ;  $0.1 \pm 0.05$  mm/mm vs  $0.18 \pm 0.09$  mm/mm;  $P = 0.15$ ;  $0.39 \pm 0.28$  vs  $0.57 \pm 0.55$ ,  $P = 0.45$ , respectively). However, significant differences were observed in the case of the ultimate tensile strength ( $2.16 \pm 0.42$  MPa and  $1.23 \pm 0.35$  MPa for the decellularized and native, respectively;  $P = 0.001$ ) and collagen phase modulus ( $8.29 \pm 2.86$  MPa and  $5.5 \pm 1.26$  MPa, for the decellularized and native, respectively;  $P = 0.04$ ), which were significantly increased in the decellularized leaflet samples compared with the native ones (Fig. 8). The increased collagen phase modulus of the decellularized tissue indicates a stiffening of the tissue following decellularization.

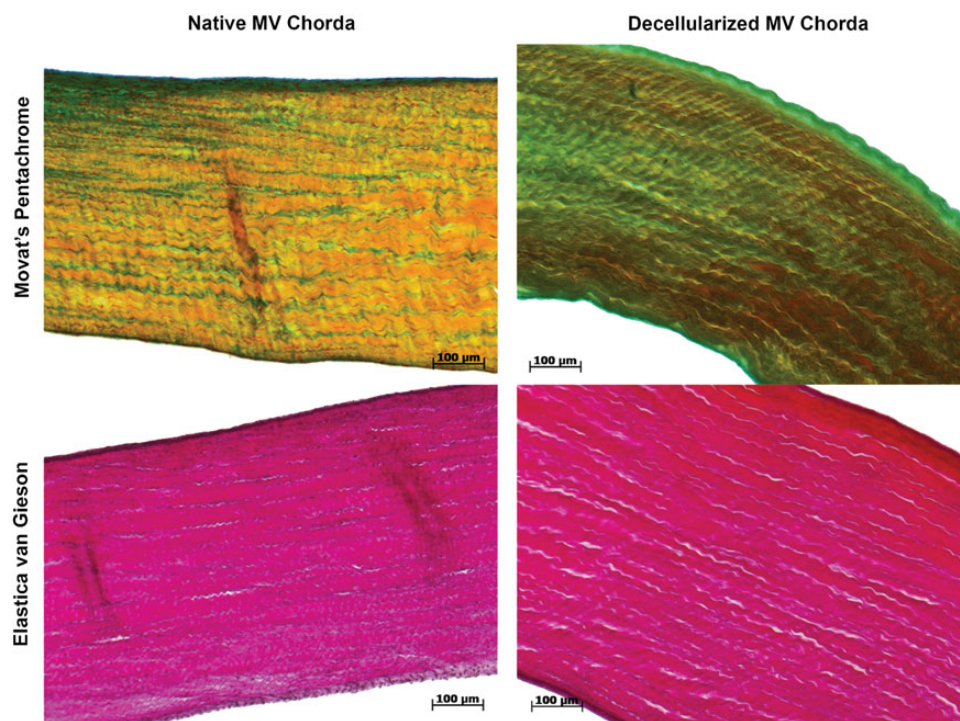


**Figure 2:** Bright-field microscopy of H&E, Movat's pentachrome and van Gieson staining of native (left) and decellularized (right) ovine MV chordae tendineae. After decellularization, the chordae demonstrated regular collagen fibres and elastin on their surface.

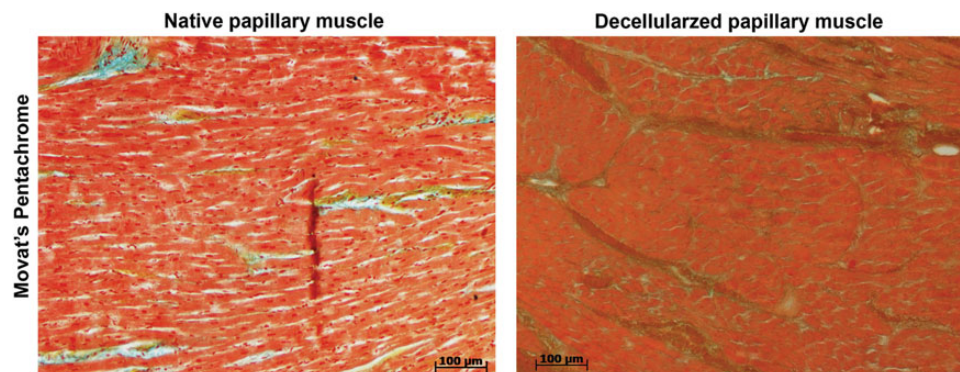


**Figure 3:** Bright-field microscopy of H&E, Movat's pentachrome and van Gieson staining of native (left) and decellularized (right) ovine MV papillary muscle. The decellularized papillary muscle demonstrated the lack of the cell nuclei.

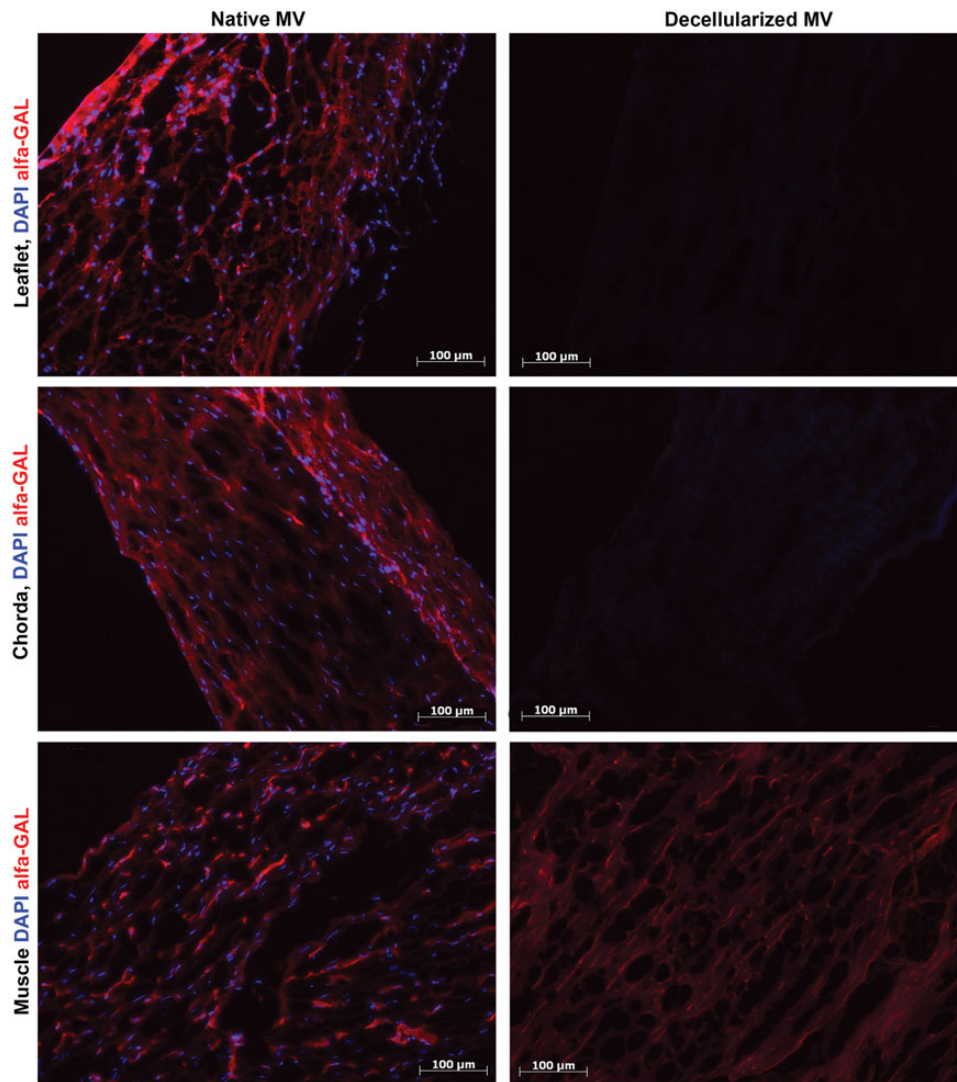


**Figure 4:** Staining of native and decellularized ovine MV leaflets, chorda tendinea and papillary muscle against nucleic acids (DAPI) and  $\alpha$ -Gal. After the decellularization, DAPI and anti- $\alpha$ -Gal antibodies fluorescence in chordae and leaflets could not be visualized, and in papillary muscles only traces of  $\alpha$ -Gal could be seen.

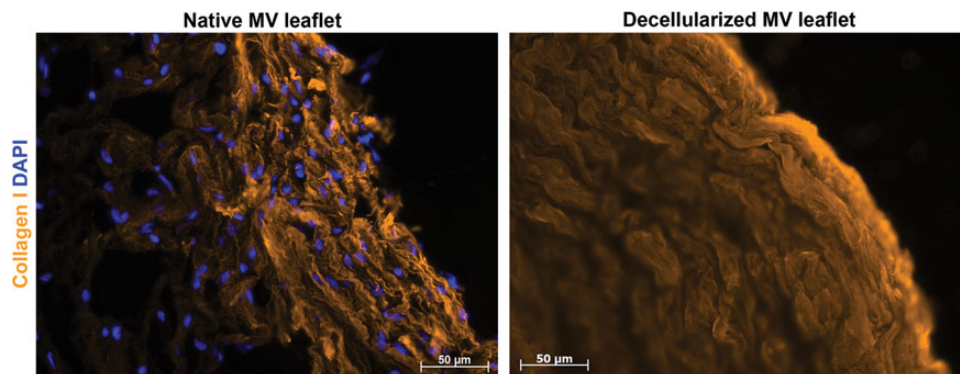


**Figure 5:** Staining of native and decellularized ovine MV leaflets, chorda tendinea and papillary muscle against nucleic acids (DAPI) and collagen I. The fluorescence of the anticollagen I antibodies shows the unchanged structure of the collagen fibres.

## DNA quantification

The amount of DNA in the native leaflets was  $287.8 \pm 76.5$  ng/mg. The DNA content in the leaflets after decellularization alone

(without DNase) was  $82.9 \pm 48.2$  ng/mg, indicating a reduction of 72%. Following DNase treatment, the DNA content in the leaflets was reduced by 96.4%, to  $10.4 \pm 16.9$  ng/mg.

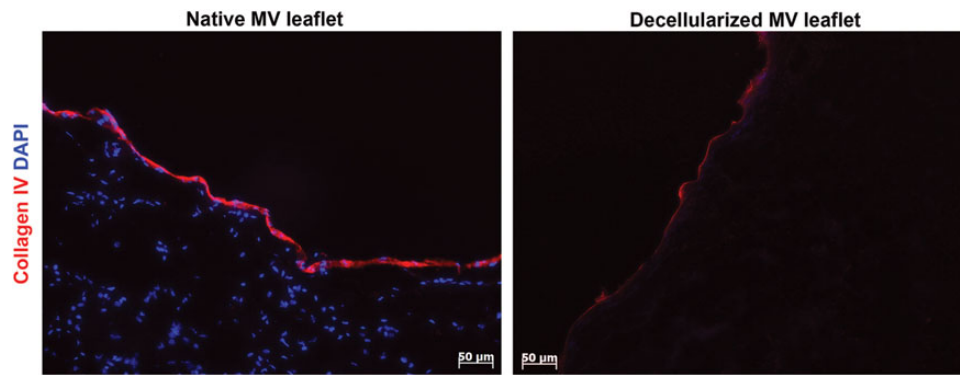


**Figure 6:** Staining of native and decellularized ovine MV leaflets, chorda tendinea and papillary muscle against nucleic acids (DAPI) and collagen IV. The collagen IV could be visualized on the entire surface of the leaflet and chordae.

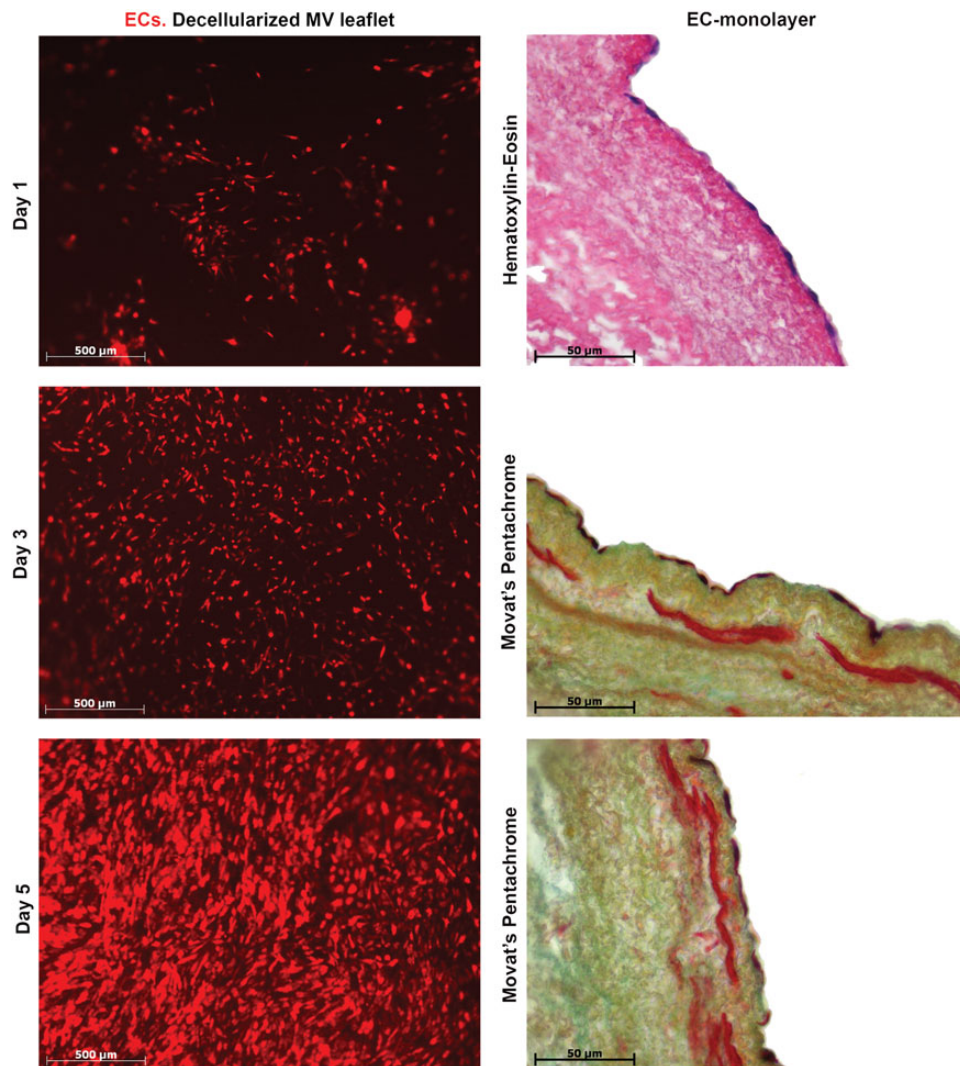


**Figure 7:** Repopulation of the decellularized MV leaflet. Left column: the photographs, showing the increasing amount of RFP-positive ECs on the leaflet's surface. Right column: bright-field microscopy of H&E and Movat's pentachrome of decellularized and reseeded MV leaflet with a monolayer of cells with endothelial morphology.

## DISCUSSION

In the last decade, several experimental studies have demonstrated reduced degeneration of decellularized homografts when compared with conventional biological grafts [15, 16]. As a consequence, several clinical studies have reported on the use of decellularized

pulmonary and aortic valve homografts, instead of cryopreserved homografts [2, 3, 9-11]. Reduced degeneration and the potential to remodel are the most remarkable properties observed after implantation of decellularized homografts in children and young adults [3]. The present study demonstrated the feasibility of producing a decellularized OMV scaffold using detergents. This

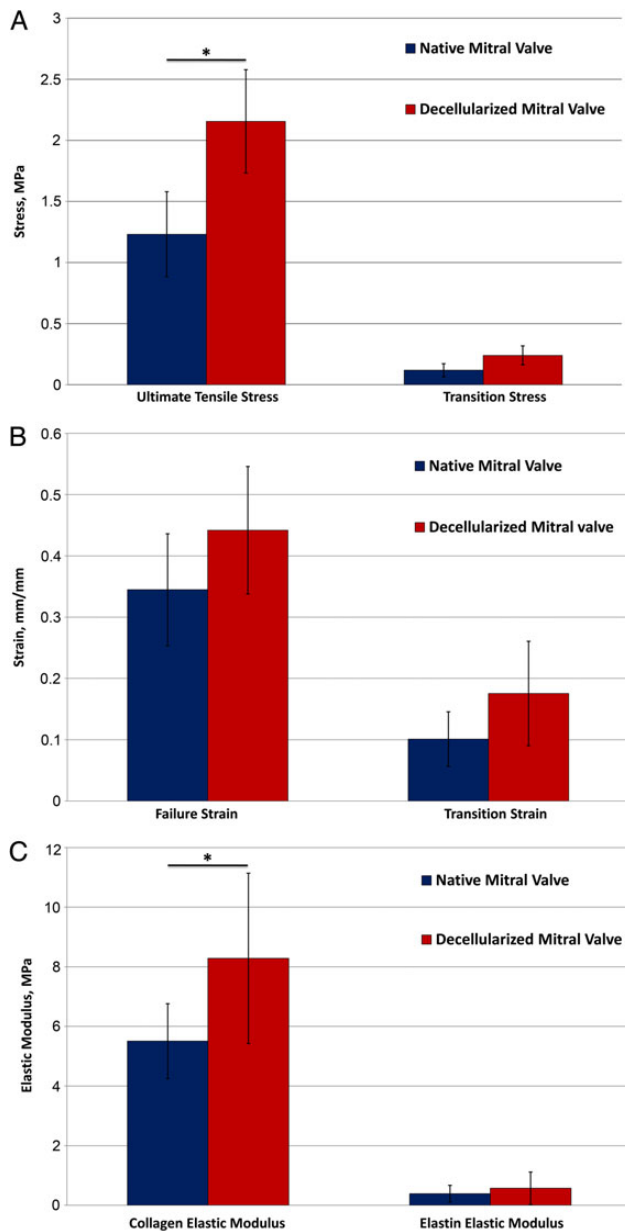


**Figure 8:** Graphics, showing the results of the mechanical tests. (A) stress characteristics, (B) strain characteristics and (C) elastic properties of native and decellularized MV leaflets. Asterisks indicate statistically significant difference.

technology can be potentially translated in the development of homograft mitral valves for clinical use, which will be of significant importance given the fact that in clinical practice there is no alternative to the biological or mechanical prostheses, which may not be suitable for selected patients with mitral valve reconstruction failure.

The decellularization protocol used in this study was based on the in-house developed protocol with SDS and SD for production of human pulmonary and aortic valve scaffolds. However, the complexity, inhomogeneity and increased thickness of the mitral valve apparatus required a more rigorous decellularization method. In order to achieve proper decellularization of the whole mitral apparatus, hypotonic preconditioning (Step 1) with distilled water was used to induce an osmotic shock to the cells, resulting in the disruption of their membranes, whereas the detergent solution was changed every 12 h throughout the decellularization process.

Moreover, the concentration of the detergents was raised gradually, allowing its slow diffusion into the tissue and the step-by-step elimination of water-soluble (below critical micelle concentration (CMC) of SDS) and lipid-soluble proteins (above CMC) [17].

A new additive,  $\beta$ -mercaptoethanol, was introduced in the decellularization protocol, as a reducing agent with the ability to increase the solubility of the proteins due to the disruption of disulfide bonds. This agent was initially used as an additive in antigen-removal solutions by Wong *et al.* [18], with some later modifications [19].  $\beta$ -mercaptoethanol disrupts the secondary and tertiary structure of the proteins by reduction of the S-S bonds, without affecting collagen I and elastin that have no disulfide bonds. Each chain of the collagen IV protein family contains three structurally distinct domains: an amino-terminal domain, a major collagenous Gly-Xaa-Yaa triple repeat and a carboxy-terminal non-collagenous (NC1) domain. The presence of cysteine- and lysine-rich residues at the aminotermisus allows the interchain crosslinking of 4 triple-helical molecules through S-S bonds and lysine-hydroxylysine crosslinks, which makes collagen IV susceptible to reducing agents. On the other hand, the main collagenous domain has interruptions, which cause additional interchain crosslinking. In addition, the NC1 domain acts as another polymerization site—here heterotrimers (two of  $\alpha$ 1-chain and one of  $\alpha$ 2-chain) form a hexamer, stabilized through extensive hydrophobic and hydrophilic interactions without involvement of any disulphide bond [20]. Thus, it was hypothesized that these types of polymerization would protect the basal membrane from  $\beta$ -mercaptoethanol. Although the intensiveness of collagen IV fluorescence decreased after decellularization to 60%, immunofluorescent staining revealed the presence of collagen IV on the entire leaflets.

The effectiveness of the decellularization method in the present study was demonstrated both by the reduction of DNA in the decellularized leaflets, which is a potential marker of intracellular antigen removal, and by the reduction of  $\alpha$ -Gal, which is the best known cell surface antigen, responsible for super-acute and acute rejection after transplantation of xenogeneic tissue. Both markers were significantly reduced in all the components of the ovine mitral apparatus, suggesting a significant reduction in both intra- and extracellular antigenicity. Moreover, detergent toxicity has been extensively investigated previously by our group [21]. Although the toxicity of  $\beta$ -mercaptoethanol is well known, it has been reported to be used in cell cultures as antioxidant. The contact cytotoxicity results in the present study demonstrated that the seeded ECs grew well into contact with the decellularized leaflets, forming a monolayer that was persistent for at least up to 7 days of culture.

The mechanical properties of the mitral valve apparatus differ significantly depending on the localization and directionality of the test sample [22]. Moreover, the test parameters, methodology and method of analysis of biomechanical testing differ significantly in the various publications [22–24]. The testing and analysis methodologies used in the present study were based on the previously reported study by Korossis *et al.* (2002) [23]. The present results for the native mitral leaflets were comparable with those published previously [23, 25]. In addition, the decreased compliance of the decellularized mitral leaflets found in the present study, was in accord with previous results on pulmonary and aortic valves decellularized with the in-house protocol incorporating SDS and SD [24]. Further *in vivo* experiments are pending with the aim of investigating the biomechanical and haemodynamic functionality of the decellularized OMV apparatus in the ovine animal model, simulating the homogeneous clinical model.

## CONCLUSION

This study demonstrated the successful decellularization of the whole mitral valve apparatus using detergents and  $\beta$ -mercaptoethanol. Although the developed method marginally affected the biomechanical behaviour of the treated leaflets, it did not impair their gross histoarchitecture. Moreover, the method reduced the cellular antigenic components in the decellularized scaffold, without affecting its cytotoxicity and, subsequently, its recellularization potential.

## Funding


This work was supported by CORTISS Hannover – Herz- und Gewebeforschungs GmbH.

**Conflict of interest:** none declared.

## REFERENCES

- [1] Kaneko T, Aranki S, Javed Q, McGurk S, Shekar P, Davidson M *et al.* Mechanical versus bioprosthetic mitral valve replacement in patients <65 years old. *J Thorac Cardiovasc Surg* 2014;147:117–26.
- [2] Brown JW, Elkins RC, Clarke DR, Tweddell JS, Huddleston CB, Doty JR *et al.* Performance of the CryoValve<sup>®</sup> SG human decellularized pulmonary valve in 342 patients relative to the conventional CryoValve at a mean follow-up of four years. *J Thorac Cardiovasc Surg* 2010;139:339–48.
- [3] Cebotari S, Tudorache I, Ciubotaru A, Boethig D, Sarikouch S, Goerler A *et al.* Use of fresh decellularized allografts for pulmonary valve replacement may reduce the reoperation rate in children and young adults. *Circulation* 2011;124:115–23.
- [4] Graham AF, Schroeder JS, Daily PO, Harrison DC. Clinical and hemodynamic studies in patients with homograft mitral valve replacement. *Circulation* 1971;44:334–42.
- [5] Kumar AS, Choudhary SK, Mathur A, Saxena A, Choy R, Chopra P. Homograft mitral valve replacement: five years' results. *J Thorac Cardiovasc Surg* 2000;120:450–8.
- [6] Nappi F, Spadaccio C, Chello M, Lusini M, Acar C. Impact of structural valve deterioration on outcomes in the cryopreserved mitral homograft valves. *J Card Surg* 2014;XX:1–7.
- [7] Shi Y, Vesely I. Characterization of statically loaded tissue-engineered mitral valve chordae tendinae. *J Biomed Mater Res A* 2004;69:26–39.
- [8] Moreira R, Gesche V, Hurtado-Aguilar LG, Schmitz-Rode T, Freze J, Jockenhoevel S *et al.* TexMi—development of tissue-engineered textile-reinforced mitral valve prosthesis. *Tissue Eng Part C Methods* 2014;20:741–8.
- [9] Da Costa FDA, Dohmen PM, Duarte D, von Glenn C, Lopes SV, Filho HH *et al.* Immunological and echocardiographic evaluation of decellularized versus cryopreserved allografts during the Ross operation. *Eur J Cardiothorac Surg* 2005;27:572–78.
- [10] Burch PT, Kaza AK, Lambert LM, Holubkov R, Shaddy RE, Hawkins JA. Clinical performance of decellularized cryopreserved valved allografts compared with standard allografts in the right ventricular outflow tract. *Ann Thorac Surg* 2010;90:1301–6.
- [11] Da Costa FDA, Costa ACBA, Prestes R, Domanski AC, Balbi EM, Ferreira ADA *et al.* The early and midterm function of decellularized aortic valve allografts. *Ann Thorac Surg* 2010;90:1854–61.
- [12] Carpentier AF, Lessana A, Relland JY, Belli E, Mihaileanu S, Berrebi AJ *et al.* The 'physio-ring': an advanced concept in mitral valve annuloplasty. *Ann Thorac Surg* 1995;60:1177–85.
- [13] Kasimir M-T, Rieder E, Seebacher G, Wolner E, Weigel G, Simon P. Presence and elimination of the xenoantigen Gal (1, 3) gal in tissue-engineered heart valves. *Tissue Eng* 2005;11:1274–81.
- [14] Vukadinovic-Nikolic Z, Andree B, Dorfman SE, Pflaum M, Horvath T, Lux M *et al.* Generation of bioartificial heart tissue by combining a three-dimensional gel-based cardiac construct with decellularized small intestinal submucosa. *Tissue Eng Part A* 2013;20:1–11.
- [15] Baraki H, Tudorache I, Braun M, Hoffer K, Gorler A, Lichtenberg A *et al.* Orthotopic replacement of the aortic valve with decellularized allograft in a sheep model. *Biomaterials* 2009;30:6240–6.
- [16] Lichtenberg A, Tudorache I, Cebotari S, Ringes-Lichtenberg S, Sturz G, Hoeffler K *et al.* In vitro re-endothelialization of detergent decellularized heart valves under simulated physiological dynamic conditions. *Biomaterials* 2006;27:4221–9.
- [17] Hayworth D. Detergents for Cell Lysis and Protein Extraction. *Protein Methods Library*. Thermo Scientific. <http://www.piercenet.com/method/detergents-cell-lysis-protein-extraction> (12 September 2014, date last accessed).
- [18] Wong ML, Leach JK, Athanasiou KA, Griffiths LG. The role of protein solubilization in antigen removal from xenogeneic tissue for heart valve tissue engineering. *Biomaterials* 2011;32:8129–38.
- [19] Wong ML, Leach JK, Athanasiou KA, Griffiths LG. Stepwise solubilization-based antigen removal for xenogeneic scaffold generation in tissue engineering. *Acta Biomaterialia* 2013;9:6492–501.
- [20] Khoshnoodi J, Pedchenko V, Hudson BG. Mammalian Collagen IV. *Microsc Res Tech* 2008;71:357–70.
- [21] Cebotari S, Tudorache I, Jaekel T, Hilfiker A, Dorfman S, Ternes W *et al.* Detergent decellularization of heart valves for tissue engineering: toxicological effects of residual detergents on human endothelial cells. *Artif Organs* 2010;34:206–10.
- [22] Grande-Allen KJ, Liao J. The heterogeneous biomechanics and mechanobiology of the mitral valve: implications for tissue engineering. *Curr Cardiol Rep* 2011;13:113–20.
- [23] Korossis S, Booth C, Wilcox HE, Watterson KG, Kearney JN, Fisher J *et al.* Tissue engineering of cardiac valve prostheses II: biomechanical characterization of decellularized porcine aortic heart valves. *J Heart Valve Dis* 2002;11:463–71.
- [24] Tudorache I, Cebotari S, Sturz G, Kirsch L, Hurschler C, Hilfiker A *et al.* Tissue engineering of heart valves: biomechanical and morphological properties of decellularized heart valves. *J Heart Valve Dis* 2007;16:567–74.
- [25] Grashow JS, Yoganathan AP, Sacks MS. Biaxial stress-stretch behavior of the mitral valve anterior leaflet at physiologic strain rates. *Ann Biomed Eng* 2006;34:315–25.

## APPENDIX. CONFERENCE DISCUSSION

 Scan to your mobile or go to <http://www.oxfordjournals.org/page/6153/1> to search for the presentation on the EACTS library

**Dr J. Kluin** (*Utrecht, Netherlands*): Your group has a large experience with decellularization of valves, and as you correctly state, the mitral valve is not only composed of leaflets but also of chords and papillary muscle. You use a slightly different decellularization protocol as compared to the aortic valves. Is that because of the papillary muscle, or what was the reason for that?

**Dr Iablonskii:** There were two reasons: first of all, the leaflets of the mitral valve are three times thicker than the aortic leaflet. The second reason is the complexity of the valve, the chordae are very dense and they need a stronger solution to be decellularized.

**Dr Kluin:** But also in the thick papillary muscle you reached full decellularization of the protocol?

**Dr Iablonskii:** Yes, we did.

**Dr Kluin:** And then you showed us the mechanical testing. I think it's only about leaflet tissue. Did you also do mechanical testing on the chords or the papillary muscle?

**Dr Iablonskii:** No, we did not. We tried to do such a test for the chordae, but it is really difficult to standardize these tests as all the chordae have different thickness and it is really difficult to compare them, that was the reason. Now we are working on a method that could make these tests possible, but it is not yet ready.

**Dr Kluin:** Some early failures in the literature were about rupture of the papillary muscle, so it would be very interesting to see what the strength of the papillary muscle is after decellularization.

**Dr Iablonskii:** Yes, we are going to test them as well.

**Dr Kluin:** You say that there is no difference in mechanical properties, but it's only in 7 animals, and when you see the figures, you might imagine that there will be a difference when you take 10 animals or 12 or so?

**Dr Iablonskii:** Yes, probably, but so far we could assume that the difference is not really high and the tendency is not towards a weakening of the tissue.

**Dr Kluin:** But towards a stronger tissue.

**Dr G. Steinhoff** (*Rostock, Germany*): You mentioned one implantation in sheep *in vivo*. Is it only one animal so far?

**Dr Iablonskii:** No, there is more than one. But the experiment is not yet finished, so it's just a preliminary report.

**Dr Steinhoff:** But primary implantation is successful?

**Dr Iablonskii:** Yes, it is.